Aust. J. Phys., 1986, **39**, 601–19

Current Status and Future Directions of Atomic Studies by Electron Spectrometry with Synchrotron Radiation*

M. O. Krause

Oak Ridge National Laboratory, P.O. Box X,
Oak Ridge, TN 37831, U.S.A.

Abstract

Representative examples of recent work on the electronic structure and dynamics of atoms are discussed and new directions in studies by electron spectrometry with synchrotron radiation (ESSR) are indicated.

1. Introduction

Electron spectrometry in combination with synchrotron radiation has proven a powerful vehicle to explore the electronic structure and dynamics of atoms, molecules and condensed matter. The use of the photoeffect as an investigative tool places the focus of the study on the properties of the target, because the number of particles in the reaction is reduced to a minimum and the perturbation introduced by the completely absorbed photon is small. The use of electron spectrometry allows for a detailed view and discrimination of virtually all the processes that occur in and between the various shells, subshells and multiplet term levels of the atom, and the vibrational levels of the simple molecules. Finally, the use of synchrotron radiation provides us with a probe of continuous tunability which is essential to reveal the dynamic behaviour of the electrons and the photon–electron interaction. Partial photoionisation cross sections σ_i and photoelectron angular distribution parameters β_i have been measured from the beginning of studies by electron spectrometry using synchrotron radiation (ESSR); spin polarisation analysis of the photoelectrons has been added more recently, and the photon range which was originally limited from about 10 to 150 eV is being extended into the keV range.

In this brief overview, only atomic species will be considered. Studies of the rare gas atoms with their closed-shell structure have reached a state of maturity. We now understand the single electron emission processes from the various subshells, and the random-phase approximation both in its nonrelativistic (RPA) and relativistic versions (RRPA) has proven to be one of the most successful theoretical descriptions. However, a number of problems remain which are now under active investigation: they concern, in particular, the dynamic behaviour of two-electron processes, especially near the thresholds, and their effects on weak subshell cross sections such as those

* Paper presented at the Specialist Workshop on Excited and Ionised States of Atoms and Molecules, Strathgordon, Tasmania, 3–7 February 1986.

0004-9506/86/050601$02.00

of s subshells. Work on other closed-shell atoms, and those with half-filled shells, is actively pursued to solidify the knowledge gained from the rare gas studies and to explore the effects peculiar to atoms with an ns^2 structure. These other atoms with subshell closure can be produced from the metallic state by vaporisation at moderate temperatures.

Work on open-shell atoms, which make up about 70% of the periodic table, has begun and will certainly be expanded in the future with the advent of more powerful photon sources and the development of high-temperature vaporisation techniques for the metals and dissociative techniques for the molecular and polymeric species of the 5B, 6B and 7B elements. Our understanding of open-shell atoms is quite incomplete and the various initial theoretical approaches remain to be tested by experiment.

In the intermediate region of the electronic structure, autoionisation resonances often dominate the photon interaction with the target over a wide spectral range. Studies of these important and often spectacular many-channel interactions are emphasised here and will doubtless receive more detailed scrutiny in the future by both theory and experiment.

Significant efforts in ESSR studies can be expected in the future in the areas of spin-polarisation analysis of the photoelectrons, photoionisation of excited states, and many-particle effects in the vicinity of innershell thresholds.

In the following discussion, recent work will be summarised and reviewed. An attempt will be made to identify the future directions for photoelectron spectrometry, which by necessity, will be used in combination with synchrotron radiation sources. Much of the background information can be found in earlier reviews (Manson 1976, 1977; Krause 1980, 1984; Wuilleumier 1981; Starace 1982; Samson 1982; Sonntag and Wuilleumier 1983; Crasemann and Wuilleumier 1985).

2. Experimental Considerations

The measurement of the energy of the photoelectron allows the determination of the atomic subshell or term level from which the photoelectron originated. The measurement of the number N_i of photoelectrons emitted into the solid angle Ω under the angle ϕ relative to the polarisation vector $p_{||}$ of polarised light allows the determination of the partial cross section σ_i and the photoelectron angular distribution parameter β_i according to the relation

$$N_i \propto \frac{\mathrm{d}\sigma_i}{\mathrm{d}\Omega} = \frac{\sigma_i}{4\pi}\{1 + \tfrac{1}{4}\beta_i(1 + 3p\cos 2\phi)\}, \tag{1}$$

where p is the polarisation of the photon beam, and where the validity of the dipole approximation has been assumed. To map out σ_i and β_i as a function of photon energy, two strategies can be employed: (1) a photoelectron spectrum (PES) is recorded at fixed photon energy and (2) a particular photoline corresponding to a given or constant ionic state (CIS) is recorded as a function of photon energy. In either mode, the dynamic properties σ_i and β_i can be determined for all processes i and for all photon energies. However, the PES spectrum is needed to reveal all the processes i and to determine the branching ratios $\sigma_i/\Sigma\sigma_i$ most accurately, while the CIS spectrum is especially useful for detailing σ_i and β_i in the region of resonances (Krause 1984). Generally, and almost invariably with metal vapours, the partial cross sections are obtained on a relative basis. They can be placed on an absolute

scale if either the densities of the target and an admixed calibrant can be determined (for example with an electro-mechanical pressure transducer in the case of permanent gases), or if the total photoionisation cross section is known and the relative σ_i of *all* processes have been measured (Wuilleumier and Krause 1974; Krause 1975). The dynamic parameters σ_i and β_i are related to basic atomic properties, namely the amplitudes and phase differences of the wavefunctions. If the spin parameters are also measured, then a complete description for the single photoionisation process in a closed-shell atom can be given in terms of the required three matrix elements and two phase differences (Heinzmann 1980).

Table 1. Value of the photoelectron angular distribution parameter β at the energy at which one of the matrix elements is zero

Subshell	β value[A]	
	$R_+ = 0$	$R_- = 0$
p; $l = 1$	0	1
d; $l = 2$	0·2	0·8
f; $l = 3$	2/7	5/7
l	$(l-1)/(2l+1)$	$(l+2)/(2l+1)$

[A] See equation (2).

Often, attention is given to the Cooper minimum which occurs when a ground state wavefunction has a node and one of the matrix elements goes to zero. In this region, the parameters are especially sensitive to the goodness of the wavefunctions, to correlation effects and to relativistic effects. The minimum in σ_i has a counterpart in a minimum in β_i; however, these minima occur at different energies. Nevertheless, the Cooper (σ) minimum can be located by a β measurement, because β for the different subshells assumes a definite value when one of the matrix elements is zero. These values are summarised in Table 1 and are based on the following relation (Manson 1976), which is valid for the dipole approximation in the independent-particle model or for closed-shell atoms:

$$\beta_i = \frac{l(l-1)R_-^2 + (l+1)(l+2)R_+^2 - 6l(l+1)R_+ \cos(\zeta_+ - \zeta_-)}{(2l+1)\{lR_-^2 + (l+1)R_+^2\}}, \qquad (2)$$

where R_+ and R_- are matrix elements for the $l+1$ and $l-1$ transitions, respectively.

Until recently, the majority of the ESSR measurements were carried out in the 10–150 eV energy range with a bandpass of typically 2 Å for the photon beam. The flux of about 10^{10}–10^{11} photons s^{-1} and the low target densities of about 10^{12} atoms cm^{-3} limited most measurements to cross sections greater than 0·1 Mb. However, as insertion devices (undulators) are coming online at existing synchrotron radiation sources and new advanced photon sources are becoming reality, studies are being (and will be) extended to higher energies (several keV), to much better resolution (that is a bandpass of 0·1–0·01 Å), and to low cross section events (in the order of kb). The inefficiency of spin polarisation measurements can then be compensated by the higher photon flux incident on the target, so that spin analysis will become as standard as are now the cross section and angular distribution measurements.

3. Subshell Properties

By its very nature, the ESSR technique probes the subshell properties. The questions then arise as to how well we understand the single-electron emission processes from the various subshells and how well theory describes the properties of the s, p, d and f electrons.

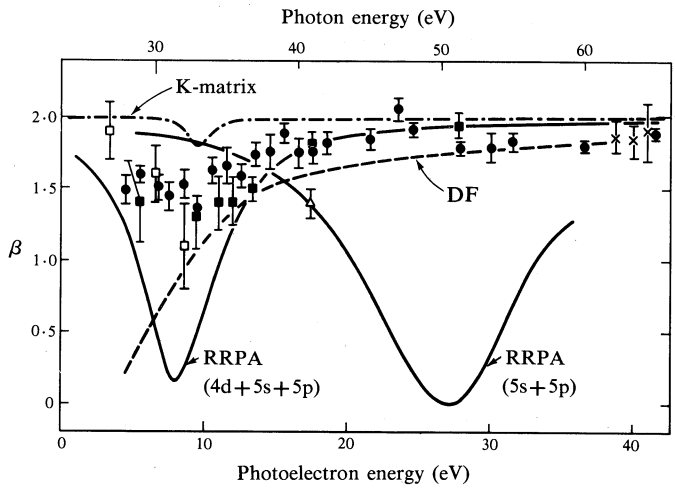

Fig. 1. The Xe 5s angular distribution parameter β in the region of the Cooper minimum. Experimental points are from Dehmer and Dill (1976) (open triangle); White *et al.* (1979) (open squares); Fahlman *et al.* (1983) (closed circles); Derenbach and Schmidt (1984) (closed squares); Southworth *et al.* (1983) (crosses). Theoretical curves are from Ong and Manson (1978) (DF); Huang and Starace (1980) (K-matrix); Johnson and Cheng (1979) (RRPA). Two predictions are not shown: the RPA (Cherepkov 1978) which predicts $\beta = -1$ in the minimum and the RTDLDA (Parpia *et al.* 1984) which is in good agreement with the data.

(a) The s Electrons

The s subshell cross sections are generally weak and are therefore subject to substantial modifications by correlation with other subshell processes and, indeed, two-electron processes. These correlations also affect the β parameter. Single-particle calculations, such as Hartree–Slater (HS) or Hartree–Fock (HF), will not suffice, and many-particle calculations which include all the important interactions must be employed. Fig. 1 shows how critical the correlations are for a prominent case, that of the Xe 5s β parameter in the region of the Cooper minimum. None of the calculations agrees well with the experimental data, not even the RRPA that considers the interactions with the 4d and 5p subshells (see e.g. Fahlman *et al.* 1983; Parpia *et al.* 1984). According to the most recent theoretical (Wendin and Starace 1983) and experimental (Fahlman *et al.* 1984) studies, the remaining discrepancy must be due to the neglect of strong two-electron transitions occurring in the $n = 5$ shell. The explicit inclusion of these transitions is yet to be undertaken. We note, however, that the relativistic time-dependent local-density approximation (RTDLDA), which includes such correlations *implicitly*, yields rather good agreement with the experiment as shown by Parpia *et al.* (1984). The neglect of the two-electron processes is also

apparent in σ(5s), especially in the region of the delayed 4d cross section maximum. Amusia (1985) has suggested to take account of this admixture of other states to the pure one-electron state by introducing a so-called spectroscopic factor which would be a constant for $h\nu \gg E_B$. The case of Xe is not unique; similar observations have been made for the outer electrons of Kr (Derenbach and Schmidt 1984), and the importance of two-electron transitions has been demonstrated for Ar (Adams *et al.* 1985).

Another case, in which the coupling of the s ionisation channel with other ionisation channels is not completely accounted for, is that of Mn. In the region of the 3p $\rightarrow$ 3d resonance, the weak 4s cross section is enhanced considerably, but theory in the multibody perturbation theory (MBPT) model underestimates the enhancement by a factor of two (Garvin *et al.* 1983; Krause *et al.* 1984).

The studies that have been made to date on the s electrons have shown the sensitivity of the s subshell properties to various correlation effects. Hence, agreement between theory and experiment is not always good. But the improvements needed are not restricted to theory alone; there is a need for experiments to be done on more atoms, over wider energy ranges, and for core s electrons where strong Coster–Kronig transitions come into play. With the availability of brighter synchrotron radiation sources in the future, these studies which are hampered now because of the weak cross sections will undoubtedly be undertaken.

(b) The p Electrons

Single-electron emission from the outer p subshells has been studied for the rare gases from threshold to about 120 eV, and occasionally up to 200 eV. Most of the measurements pertain to the β parameter and to the intensity ratio of the spin–orbit doublet. Generally, the data are in good accord with the predictions of the RPA (Amusia *et al.* 1972), RRPA (Johnson and Cheng 1979) and RTDLDA (Parpia *et al.* 1984), provided all major correlations are taken into account. The accord between theory and experiment is illustrated in Fig. 2 for the Xe 5p β parameter (Southworth *et al.* 1983) and in Fig. 3 for the $\sigma(5p_{3/2})/\sigma(5p_{1/2})$ intensity ratio (Krause *et al.* 1981). The neglect of two-electron transitions in the calculations is not serious for p electrons, as it is for s electrons, because the p subshells have substantial cross sections. However, these correlations are present and their inclusion in the many-body models would undoubtedly further improve the agreement. Studies of σ and β have recently been augmented by measurements of the spin parameters α and A (Heckenkamp *et al.* 1984). As for σ and β, the spin analysis data reported for the $5p_{3/2}$ and $5p_{1/2}$ electrons of Xe between 13 and 30 eV are in good agreement with the RRPA results.

Investigations of inner p electrons have begun, and β parameters and relative cross sections have been reported for the Kr 3p subshell up to $h\nu = 800$ eV (Lindle *et al.* 1986). For these core electrons with $l = 1$, correlation effects were found to be unimportant. However, the absence of many-body effects for inner p subshells with nearby d subshells is not always assured, as seen most dramatically in the case of the Xe 4p (Wendin and Ohno 1976) and Th 5p (Wendin 1982) electrons.

As examples of metal vapour work, outer p electrons have been examined in Pb (Krause *et al.* 1986) over a small energy interval and inner p electrons in Hg (Kobrin *et al.* 1983) over a wider energy range. In the case of Hg 5p, the data on σ and β and the spin–orbit intensity ratio were observed to be in satisfactory agreement with DS calculations, but only in fair agreement with the RRPA calculations. This result

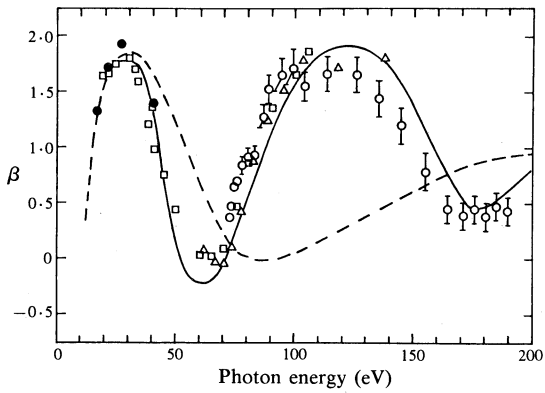

Fig. 2. Photoelectron angular distribution parameter β for the Xe 5p subshell. [From Southworth *et al.* (1983).]

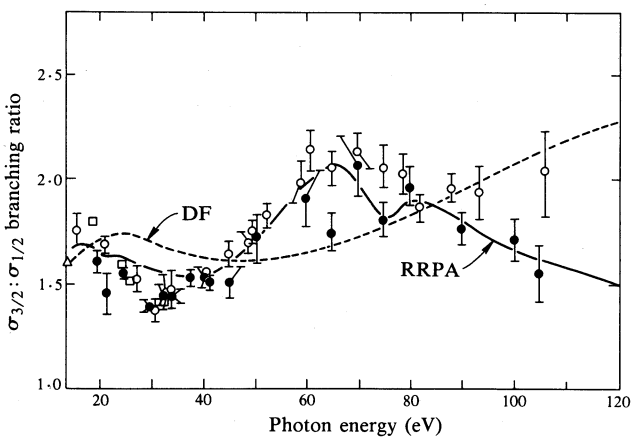

Fig. 3. Intensity ratio for the Xe 5p spin–orbit components. [From Krause *et al.* (1981).]

might indicate that the various channel interactions effectively cancel each other and that the RRPA calculation did not consider enough channels to effectuate this cancellation.

Present and past work on the properties of the p electrons indicates that, although the situation is quite satisfactory for the outer p electrons of the rare gases, future efforts will be directed towards p electrons in open-shell atoms to map out the properties over the entire periodic table. Intense efforts can be expected to be directed toward the halogens and chalcogens; initial σ measurements have already been reported for the 2p level of atomic oxygen (Samson and Pareek 1985; Hussein *et al.* 1985).

(c) The d Electrons

The least bound d electrons have been investigated in a number of cases, for example, Kr 3d (Lindle *et al.* 1986), Xe 4d (West *et al.* 1976), Ag 4d (Krause *et al.* 1985), Au 5d (Schmidt 1985), Hg 5d (Kobrin *et al.* 1983) and Pb 5d (Krause *et al.*

1986). Theory, especially the RRPA model, is seen to reproduce the experimental observations quite well in most instances. A surprisingly large discrepancy occurs for Xe 4d (West *et al.* 1976; Schmidt 1985) where the RPA and RRPA calculations overestimate σ at the position of the delayed maximum by about 25%. For the d subshell, a good theoretical result for σ and β presupposes an accurate assessment of the centrifugal barrier acting on the escaping photoelectron. But correlation effects and, of course, relativistic effects also play a role as evidenced most clearly in the intensity ratio of the spin–orbit components. Recent results on this intensity ratio in Xe (Yates *et al.* 1985) and in Hg (Kobrin *et al.* 1983) show a satisfactory overall agreement with the RRPA predictions, but the corresponding data for the Kr 3d subshell (Aksela *et al.* 1985) are at variance with the RRPA results. Future work will surely resolve these discrepancies; and future work will also be extended to open-shell atoms in which the properties of the multiplet components can be examined. Good candidates are of course the 3d and 4f transition series elements and 4B atoms.

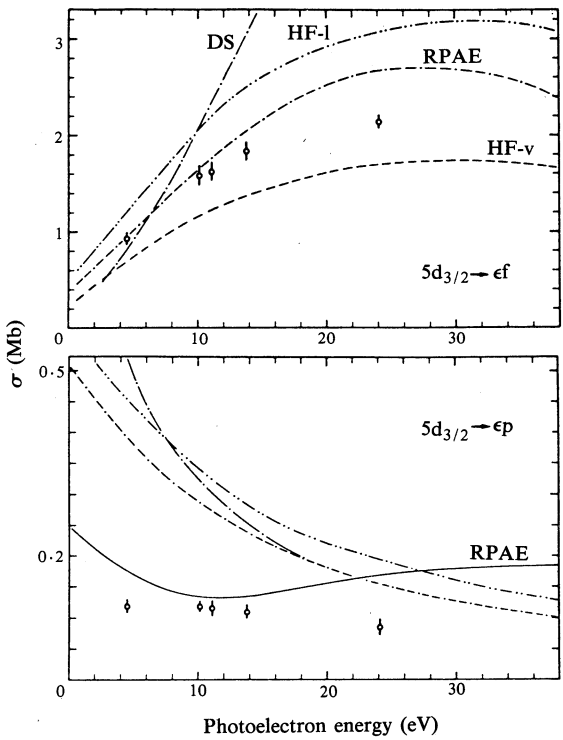

Fig. 4. Partial cross sections for the ϵf and ϵp channels of $5d_{5/2}$ photoionisation in Hg. [From Schönhense and Heinzmann (1984).]

In Section 3*a* on s electrons, the importance of interchannel interactions on weak cross sections was pointed out. Such correlations should also be important for the $l-1$ transitions which are generally weak. In an experiment using spin analysis, the interaction between the strong $5d_{3/2} \rightarrow \epsilon f$ and the weak $5d_{3/2} \rightarrow \epsilon p$ channel could in fact be demonstrated for the 5d subshell of Hg (Schönhense and Heinzmann 1984). Fig. 4 shows that the monotonic decrease of $\sigma(d_{3/2} \rightarrow \epsilon p)$, which is expected in the single-particle picture, does not occur due to the coupling with the $d_{5/2} \rightarrow \epsilon f$ channel.

(d) The f Electrons

Only two studies have been reported so far, one for the Hg 4f subshell (Kobrin *et al.* 1983) and one for the Yb 4f subshell (Svensson *et al.* 1986). Both atoms have a closed-shell structure and, hence, RRPA calculations exist which allow a comparison with experimental data. The β values for the Hg 4f components and the σ and β values for the Yb 4f doublet were found to be in good agreement with the RRPA results. This, together with the results for the s, p and d electrons, leads to the significant conclusion that this theoretical model, which taking into account both relativistic and many-body effects represents one of the most advanced models, is capable of predicting the dynamic parameters for all subshells with generally good accuracy.

4. Two-electron Photoionisation Processes

Two-electron transitions as manifested in the so-called correlation satellites, which accompany the single-electron photolines in a photoelectron spectrum, were investigated in the early phases of photoelectron spectrometry (Krause 1975, 1980) and have come into renewed focus recently. Their study is of intrinsic interest because they are the most direct evidence of electron correlation, but their study is also important because they influence the single-electron properties discussed in Section 3. Present work is concentrating on the behaviour of the two-electron processes near threshold and somewhat above it. Both σ and β determinations of the satellite lines contribute to the assignment of the states involved and the origin of the satellites in terms of electron–electron interactions in the atomic ground state, the ionic final state and the continuum channels. The energy dependence of σ for the satellites provides the criterion for the relative energy at which the sudden approximation becomes valid and the regime in which the idea of the spectroscopic factor mentioned in conjunction with s electron ionisation can be applied.

Extensive results have been reported for the valence photoelectron satellites in Ne (Heimann *et al.* 1985), and the major K shell satellites have been studied in Ne and Ar (Kobrin *et al.* 1984). The latter work extended the use of photon energies from the synchrotron radiation source into the keV range, a range which will be increasingly utilised in the future for satellite studies and studies of other processes occurring in the neighbourhood of core electron levels (Armen *et al.* 1985*b*). In a related investigation, Auger electrons were used to determine the relative intensities of two-electron processes in the KL shells of argon (Armen *et al.* 1985*a*). It may be recalled at this point, that Auger electron satellites can give access to both shakeup (ϵ, n) and shakeoff (ϵ, ϵ) processes, while the photoelectron lines give evidence of ϵ, n processes only. The ϵ, ϵ processes, in which two electrons go into the continuum, amount to typically 10% of the single ionisation event and presumably exert a small influence on the single-electron properties discussed in Section 3. In conjunction with Ar 3s (Adam *et al.* 1985), Kr 4s (Derenbach and Schmidt 1984) and Xe 5s (Fahlman *et al.* 1984) ionisation, correlation satellites were measured in the region of the ns Cooper minima. States that are reached by direct two-electron photoionisation can also be populated indirectly by autoionisation in certain energy regions. The often spectacular effects in the resonance regions will be discussed in Section 7.

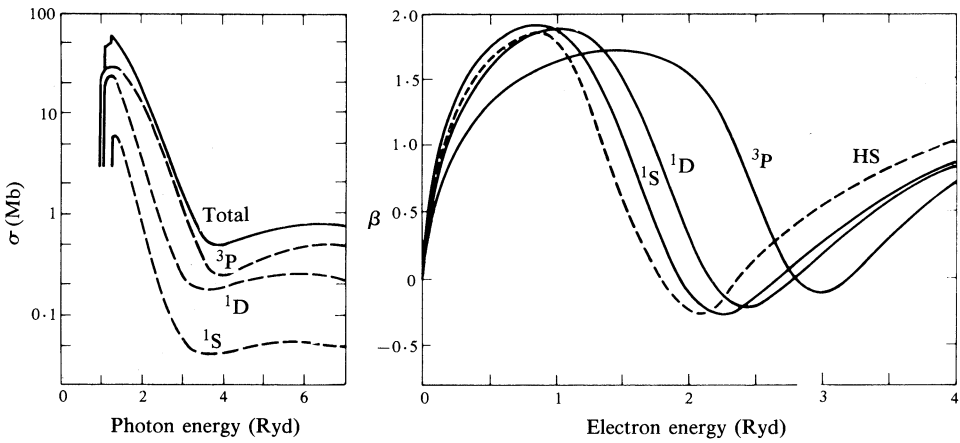

Fig. 5. Theoretical partial cross sections and β parameters for the multiplet components of the 3p subshell of Cl as an example for a p^5 element (1Ryd = 13·605 eV). [From Manson *et al.* (1979).]

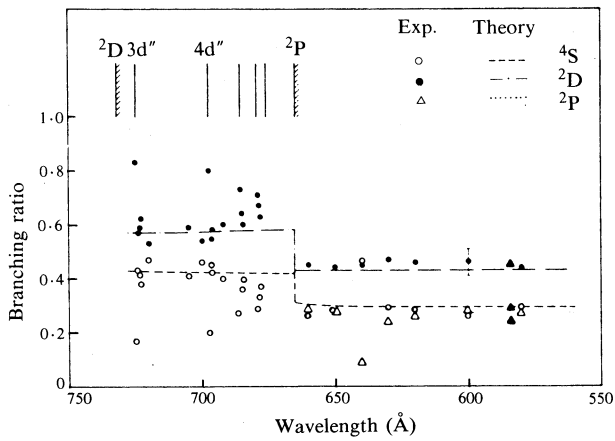

Fig. 6. Branching ratios for atomic oxygen. [From Hussein *et al.* (1985).]

5. Open-shell Atoms

Much of the work carried out so far has been on closed-shell atoms and much of the material presented on the various subshells in Section 3 concerned atoms with closed-shell structure. Open-shell atoms are essentially a new area for both experimental and theoretical study. Generally, these atoms require higher temperatures for preparation and a greater effort for analysis than the closed-shell atoms. Similarly, the complexity of the theoretical treatment increases dramatically. However, these difficulties are being overcome, and the coming years will see a combined experimental and theoretical attack on open-shell elements which make up the larger part of the periodic table. On the experimental side, the availability of brighter photon sources and high-resolution monochromators will be crucial, and on the theoretical side, the development of efficient calculational procedures will be important for rapid progress.

Pilot studies have already been undertaken. This work focused, naturally, on the dynamic behaviour of the multiplet term components. Theoretical predictions for the dynamic properties of the Cl 3p levels are shown in Fig. 5 (Manson *et al.* 1979), and the measured branching ratios for the oxygen 2p terms are presented in Fig. 6 (Hussein *et al.* 1985). Few other measurements outside resonance regions exist at the present time; in one of the recent studies, $\sigma(^2P_{1/2})$ and $\sigma(^2P_{3/2})$ of the 6p electrons of Pb were measured over a wider energy range (Krause *et al.* 1986); in another study, the β parameter was determined for two term components of the Pb 5d multiplet (Derenbach *et al.* 1984), and finally, the partial cross sections for all the term levels resulting from 1s ionisation of Li were measured up to 115 eV (Gerard *et al.* 1986).

Instead of producing free atoms by vaporisation from their metals or by dissociation of diatomic molecules or polymeric species, singly and multiply charged rare gas ions can be used to mimic open-shell atoms. For example, Ar^{1+} is isoelectronic with Cl and Kr^{2+} with Se. Ions may very well play a major role in the research of open-shell atoms; a first ion beam experiment has already been carried out on Ba^+ in the region of a resonance of high cross section (Lyon *et al.* 1984). Of course, research with ions, which are important in plasma and astrophysics, has its own intrinsic interest. For example, the quality of atomic calculations can be tested by way of the ionic Cooper minima over a greater variety of electronic structures and nuclear fields than those possible with neutrals (Yin and Pratt 1985).

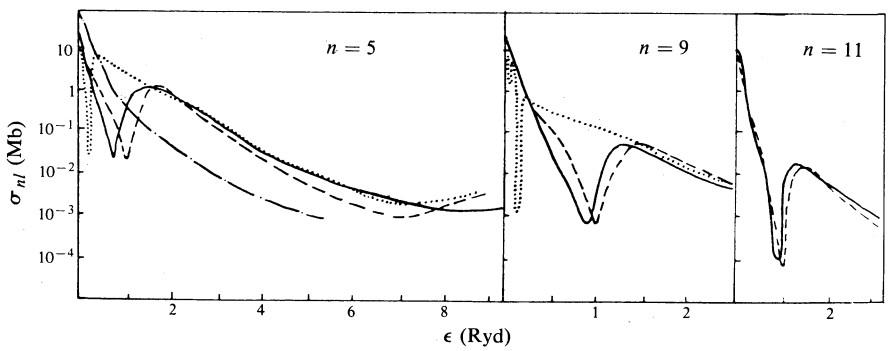

Fig. 7. Photoionisation cross sections for the Cs nd(^{2}D) excited states. Solid curves are RPA results; dashed, dotted and chain curves are HF, HS and Coulomb approximation results, respectively. [From Avdonina and Amusia (1983).]

6. Excited States

Recent pioneering experiments (Wuilleumier 1982; Nunnemann *et al.* 1985; Bizau *et al.* 1985) in which two modern research tools, synchrotron radiation and laser light, are combined have shown us that it is now possible to embark on comprehensive studies of excited atomic states. Although σ of the excited states is usually large, the effective target density is small due to the required *double-beam* excitation conditions. The absolute cross section of the Na 3p excited state has been reported (Preses *et al.* 1985) and σ of Ba 5d has been measured as a function of photon energy (Bizau *et al.* 1986). Other properties of the excited states in these and other atoms remain to be elucidated and the theoretically predicted multiple Cooper minima and their positions (Lahiri and Manson 1982; Avdonina and Amusia 1983) need to be confirmed by

experiment. As seen in Fig. 7 for Cs nd(^{2}D), and known from ground-state atoms, the position of the Cooper minimum is extremely sensitive to the model potential chosen.

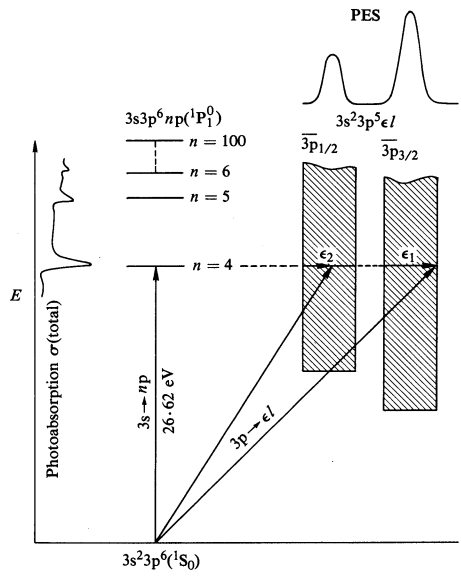

Fig. 8. Schematic representation and energy diagram for the Ar 3s autoionisation resonance in which two continuum channels can be populated.

7. Autoionisation Resonances

Autoionisation resonances are a common event in the energy regime from 10 eV to about 300 eV. This energy regime contains many energy levels, which increase in number with increasing atomic weight. Because some of these levels or subshells may be empty or partially filled, as for example in transition series elements, transitions from nearby filled subshells to these empty levels will be strong and will inevitably compete and, in fact, interfere with transitions to the continuum from less tightly bound levels. This channel interaction, which is called autoionisation, results in often spectacular resonances as the electron structure responds to an external perturbation. As a reminder, a schematic representation of autoionisation is given in Fig. 8 for the resonance in argon at 26·62 eV, at which energy the continuum transitions 3p $\rightarrow$ ϵl interfere with the discrete transitions 3s $\rightarrow$ 4p. The resulting resonance can be observed in the photoabsorption cross section or in the partial photoionisation cross sections, the photoelectron angular distributions and the photoelectron spin parameters of the indicated exit or continuum channels.

A great many autoionisation resonances have been studied through the years using various techniques (and observables) and excitation modes. An excellent survey of the field, with an emphasis on modern theoretical and experimental developments, can be found in the Proceedings of a recent workshop on the subject (Berry *et al.* 1985). A fair number of systems have been investigated in recent years by the ESSR technique. The anticipated improvements in this technique, especially higher

resolution and greater brightness of the photon source, will doubtless lead to many more studies in the future. Detailed measurements of σ, β and spin parameters for all exit channels of the resonance states are possible and are needed for a good understanding of the channel interactions. By the very nature of the problem, the theoretical treatment is very difficult, especially when many channels are involved, and interplay with experiment will help to identify the most important interactions and to sort out the most efficient approaches.

In the rare gases, the favourites of atomic research, many of the existing resonances were delineated by measuring σ and β, and even spin polarisation, for individual channels. The variation of σ and β for the exit channel associated with the $He^+(n = 2)$ state was determined over the resonance region that leads up to the $n = 3$ threshold (Lindle *et al.* 1985). It should be noted, that these ESSR data are in good agreement with fluorescence data (Woodruff and Samson 1982) and with MBPT results (Salomonson *et al.* 1985). The Ar 3s (Codling *et al.* 1980; Svensson 1985), Kr 4s and Xe 5s (Ederer *et al.* 1982) resonances were characterised by σ and β of the two available exit channels indicated in Fig. 8 for the case of Ar. Photoelectrons emitted in the autoionisation region between the 4p spin–orbit levels of Kr were subject to spin analysis and the data (Heinzmann and Schäfers 1980) were seen to be in good agreement with RRPA calculations (Johnson *et al.* 1980). At present, these as well as other electron emission measurements lack the resolution that is desirable and which could be achieved in total absorption (Connerade 1983) and ion yield measurements (Berkowitz 1979). A deeper lying resonance arising from the Xe(4d $\rightarrow$ *n*p) excitations was studied by way of the partial strengths (σ) of the $5p_{3/2}$, $5p_{1/2}$ and 5s channels (Southworth *et al.* 1983; Becker *et al.* 1986*b*). In addition, the Auger channel that opens up for this inner-shell excitation was also observed in one of the studies (Southworth *et al.* 1983).

While resonances are restricted to rather narrow energy intervals in the case of the rare gases with their closed-shell structure, autoionisation in the closed-shell atom Yb extends over a wider energy range and dominates this spectral region (Svensson *et al.* 1986). It is the proximity of the empty 5d subshell to other subshells in the intermediate region of the electronic structure that allows strong 5p $\rightarrow$ 5d transitions and rapid autoionisation involving the $4f_{5/2}, \epsilon l$; $4f_{7/2}, \epsilon l$; and 6s, ϵp continuum channels. Auger channels are added at the higher energies, but these channels and their coupling with the other continuum channels are yet to be studied systematically.

In open-shell atoms, autoionisation resonances are likely to dominate the photon–atom interaction over a wide spectral range. A prime example is offered by $Mn(3p^6 3d^5 4s^2)$ in which the 3p $\rightarrow$ 3d resonance strongly modifies the total and partial cross sections and the β parameters from about 30 to 80 eV (Bruhn *et al.* 1982; Kobrin *et al.* 1984; Krause *et al.* 1984; Schmidt *et al.* 1985). The strong effects on σ(3d), σ(4s), σ(satellites) and β(3d) are displayed in Fig. 9 using one of the data sets and one of the theoretical calculations, namely the MBPT prediction (Garvin *et al.* 1983). How crucial it is to extend the measurements over all exit channels, including the weaker two-electron channels, can be seen from Fig. 10. The spectra of Fig. 10 clearly demonstrate that the structure observed in the absorption spectrum of Mn between 55 and 58 eV is associated with autoionisation processes involving $3d^4(^5D)4s, nl, \epsilon l$ channels which appear in a photoelectron spectrum as correlation satellites. Detailed recordings of such low cross section processes require a special effort at the present time, but with future instrumental improvements will become

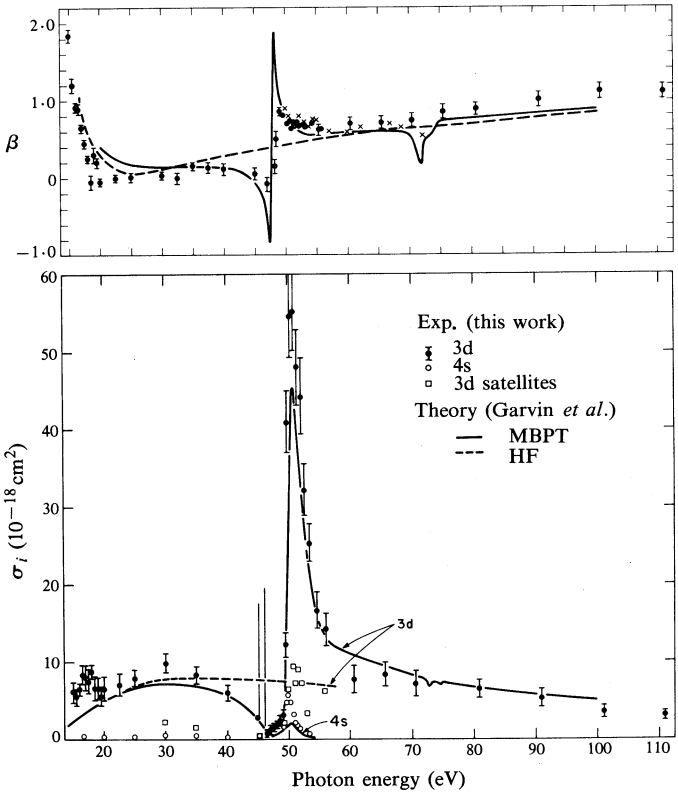

Fig. 9. Effect of the 3p→ 3d resonance in Mn on the partial cross sections and the 3d β parameter. Note that the resonances appearing in the MBPT calculation near 56 eV are omitted in this plot. [From Krause *et al.* (1984).]

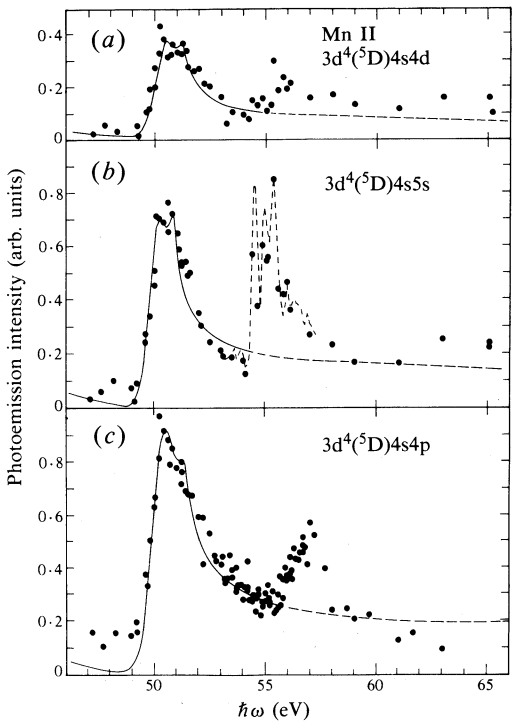

Fig. 10. Role of the main two-electron processes corresponding with correlation satellites in the PES over the 3p→ 3d resonance region in Mn. The resonances near 56 eV are exclusively associated with these higher order transitions. The dashed curve in (*b*) represents a CIS measurement and shows the power of this mode of operation to reveal detailed features. [From Schmidt *et al.* (1985).]

a matter of 'routine' allowing us to systematically advance our understanding in interplay with theoretical analyses.

The 3p → 3d resonances have been examined across the 3d transition series, namely for the elements Cr, Fe, Co and Ni (Schmidt 1985). However, only σ values and no β values have been reported so far, and corresponding theoretical calculations are still lacking.

Proceeding beyond the 3d series, Ga($3d^{10}4s^24p$) was chosen to measure σ and β of the three exit channels for the 3d → 4p resonance (Krause *et al.* 1983*a*); and Cu($3d^{10}4s$) was used to reveal the effects of the 3p → 4s resonance on correlation satellites leaving Cu^+ in the $3d^84s^2$ states (Chanderis *et al.* 1981). The latter work played a decisive role in an all-out effort to identify the origin of a low-energy resonance observed in the Ni metal.

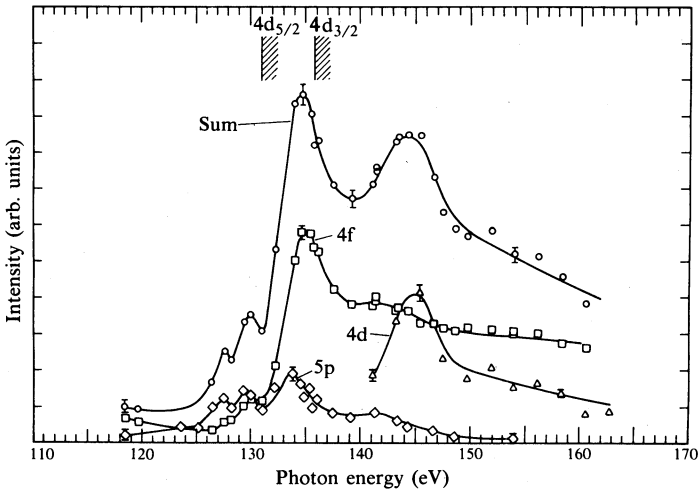

Fig. 11. Relative partial strengths of the exit channels and their sum in the neighbourhood of the 4d → 4f resonance in Sm. [From Prescher *et al.* (1986).]

Analogous to the 3p → 3d resonances of the 3d elements, 4d → 4f resonances, and indeed 3d → 4f resonances, of the rare earths elements have a pronounced influence on the response of the electronic structure to an electromagnetic perturbation. Data have been presented most recently for Eu($4f^76s^2$) (Becker *et al.* 1986*b*) and Sm($4f^66s^2$) (Prescher *et al.* 1986). The partial cross sections σ(4d), σ(4f), σ(5p) and their sum are presented in Fig. 11 for Sm. While the behaviour of σ for Eu is reminiscent of the trends observed for Mn (see Fig. 9), the trends for Sm differ somewhat by the occurrence of a double hump structure in σ(tot). The measurement of the partial channels reveals that the resonance near 135 eV is linked with the 4f,ϵl and 5p,ϵl exit channels while the resonance at about 145 eV primarily decays into the 4d,ϵl channel. The experiments on Sm and Eu represent the first work on the strong 4d → 4f resonance in the lanthanide series.

As a representative of the heaviest elements that can be produced conveniently as atomic vapours, Pb has been studied over the 6p resonance, which gives evidence of

the admixed $6p_{3/2}$ state, and over the 6s and the 5d resonances. Out of this work, the $6s \rightarrow 7p_{3/2}$ resonance is shown in Fig. 12, illustrating the behaviour of σ for the two available exit channels (Krause *et al.* 1983*b*). The channel interactions are such that a Lorentzian resonance appears in the $6p(^2P_{3/2}), \epsilon l$ channel and a window resonance in the $6p(^2P_{1/2}), \epsilon l$ channel. Both resonances have nearly equal *absolute* intensity. As a result, this resonance state could not be observed in absorption in which the contributions from the exit channels are automatically summed up. Although complete cancellation is probably rare, partial cancellation is probably not uncommon and has been observed in other cases, as for example in $Cd(4d^{10}5s^2)$ in which the 4d, ϵl channel displays a window profile, the 5s, ϵp channel a medium-q Fano profile, and the 5p, ϵl channel high-q (Lorentzian) profile at the position (588 Å) of the $4d^9 5s5p6s$ resonance (Kobrin *et al.* 1982).

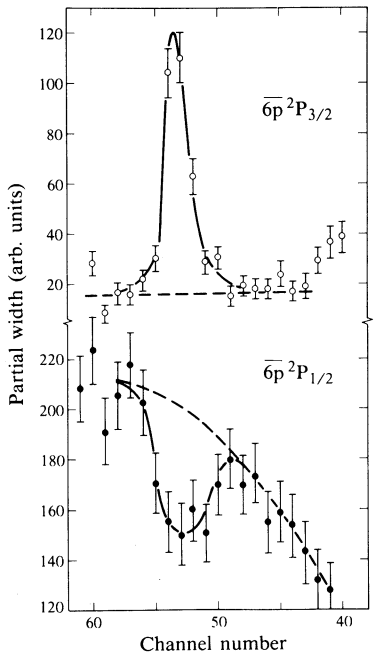

Fig. 12. The $6s \rightarrow 7p_{3/2}$ autoionisation state in Pb showing a Lorentzian and a window resonance of nearly equal magnitude in the two available exit channels. [From Krause *et al.* (1983*b*).]

Two-electron excitations that populate continuum channels identifiable in a PES spectrum by the correlation satellites are very common in atoms with a ns^2 outer configuration. The first evidence for this type of process was presented for $Ba(5p^6 6s^2)$ in which the autoionising $5p^6 6s^2 \rightarrow 5p^5 5d6s5d$ transition competes with the direct transition from $5p^6 6s^2$ to the final continuum state $5p^6 5d$, ϵl (Rosenberg *et al.* 1979). As a consequence, the normally weak PES satellite corresponding to the emission of a 6s electron with the simultaneous promotion of the other 6s electron to the 5d level ($6s^2 \rightarrow 5d$, ϵl) is much enhanced by the autoionisation resonance involving the excitation of a 5p6s electron pair.

A multitude of resonance phenomena have been observed in the photoelectron spectra of $Ca(4s^2)$ excited in the 3p threshold region (Bizau *et al.* 1984). The observation could be classified into single-electron and double-electron (and even

triple) excitations and further distinctions could be made within the decay channels, which could either be of the autoionisation type $3p^5 4s^2 nl \rightarrow 3p^6 4s\epsilon l$, or the Auger type $3p^5 4s^2 nl \rightarrow 3p^6 4s n'l'\epsilon l$ or a combination of the two for the various resonance states.

In a spin polarisation measurement of an atomic vapour the exit channels of the autoionisation resonances above the Hg 6s threshold were resolved into the singlet and triplet components (Schönhense *et al.* 1984).

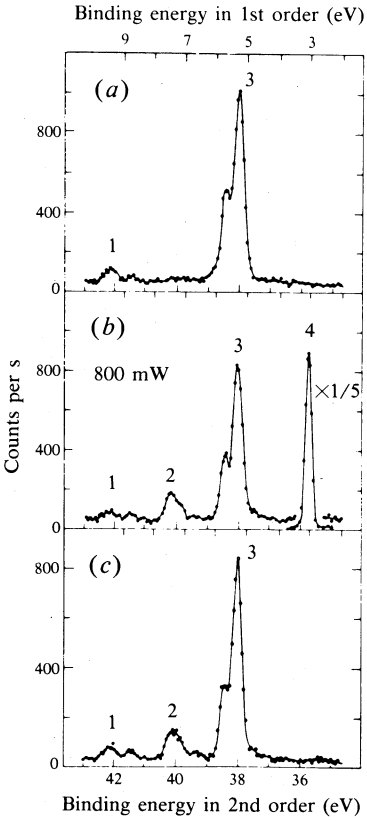

Fig. 13. Photoelectron spectrum of Na under different experimental conditions, showing (*a*) the 2p photolines in neutral Na($2p^6 3s$) excited by 65·46 eV photons; (*b*) the 2p photolines in the laser excited Na*($2p^6 3p$) produced by 32·73 eV photons at the position of the 2p→ 3s resonance, and 2p photolines in the residual neutral Na; (*c*) the same source conditions as for (*b*), but with excitation off-resonance ($h\nu = 32{\cdot}50$ eV). This shows that peak 2 corresponds with 2p ionisation in Na*, peak 3 with 2p ionisation in Na and peak 4 with a resonance state. [From Bizau *et al.* (1985).]

Autoionisation resonances in *excited* atoms have recently been reported for Na (Bizau *et al.* 1985) and Ba (Nunnemann *et al.* 1985). In these cases, the excited state was produced by laser irradiation and the resonance was probed by photons from a synchrotron radiation source. These are pilot experiments of a new genre and we should see many more in the future with the expected technical advances in the various experimental techniques. In the case of Na, the excited atom $2p^6 3p(^2P)$ was promoted to the autoionisation states $2p^5(^2P)3s3p(^{1,3}P)^{2,4}S$, $^{2,4}P$, $^{2,4}D$; and the decay to $2p^6(^1S)+e$ was observed as shown in Fig. 13. In the case of Ba, the laser produced excited atom $5p^6 6s6p(^1P_1)$ was investigated in the autoionisation region of $5p^6 6s5d(^{1,3}D)6s6p(^1P)$ by determining the population of the various final states observable in the PES spectrum in the binding energy range from 3 to 14 eV.

8. Conclusions

An overview of the current status of the field has been given and areas that are likely to be emphasised in coming years have been identified. Most of the future directions of ESSR studies of atoms are closely tied to instrumental improvements. These improvements are being initiated now. With their completion we will be able to explore systems and processes that have eluded scrutiny so far, and advance our knowledge and understanding of the electronic structure and dynamics of atoms. Specifically, we might expect a concentration of effort to occur in the investigations of open-shell atoms, excited atoms, and ionic species. Studies will increasingly include spin polarisation measurements and they will emphasise many-body effects, which are responsible for the ubiquitous autoionisation resonances, the photoelectron satellites and phenomena occurring in the vicinity of inner-shell ionisation thresholds.

Acknowledgments

The Specialist Workshop, where this paper was presented, was sponsored, in part, by the U.S. National Science Foundation under Grant No. INT-85-14710. This work was supported by the Division of Chemical Sciences, Office of Basic Energy Sciences, U.S. Department of Energy under contract DE-AC05-840R21400 with the Martin Marietta Energy Systems, Inc.

References

Adam, M. Y., Morin, P., and Wendin, G. (1985). *Phys. Rev.* A **31**, 1426.

Aksela, S., Tan, K. H., Bancroft, G. M., Aksela, H., Yates, B. W., and Coatsworth, L. L. (1985). *Phys. Rev.* A **32**, 1219.

Amusia, M. Ya. (1985). *Comments At. Mol. Phys.* **16**, 143.

Amusia, M. Ya., Cherepkov, N. A., and Chernysheva, L. V. (1972). *Phys. Lett.* A **40**, 15.

Armen, G. B., Åberg, T., Karim, K. R., Levin, J. C., Crasemann, B., Brown, G. S., Chen, M. H., and Ice, G. E. (1985*a*). *Phys. Rev. Lett.* **54**, 182.

Armen, G. B., Åberg, T., Levin, J. C., Crasemann, B., Chen, M. H., Ice, G. E., and Brown, G. S. (1985*b*). *Phys. Rev. Lett.* **54**, 1142.

Avdonina, N. B., and Amusia, M. Ya. (1983). *J. Phys.* B **16**, L543.

Becker, U., Kerkhoff, H. G., Lindle, D. W., Kobrin, P. H., Ferrett, T. A., Heimann, P. A., Truesdale, C. M., and Shirley, D. A. (1986*a*). *Phys. Rev.* A **34** (to be published).

Becker, U., Schmidt, E., Sonntag, B., and Wetzel, H. E. (1986*b*). *Phys. Rev.* A **33**, 3891.

Berkowitz, J. (1979). 'Photoabsorption, Photoionization and Photoelectron Spectroscopy' (Academic: New York).

Berry, H. G., Berkowitz, J., and Berry, R. S. (Eds) (1985). Proc. Workshop on Some Aspects of Autoionisation in Atoms and Small Molecules. Rep. ANL-Phy-85-3, Argonne National Laboratory, Argonne, Illinois.

Bizau, J. M., Cubaynes, D., Gerard, P., Wuilleumier, F., Keller, J. C., LeGouët, J. L., Picqué, J. L., Ederer, D. L., Carré, B., and Wendin, G. (1986). *Phys. Rev. Lett.* **57**, 306.

Bizau, J. M., Gerard, P., Wuilleumier, F., and Wendin, G. (1984). *Phys. Rev. Lett.* **53**, 2083.

Bizau, J. M., Wuilleumier, F., Ederer, D. L., Keller, J. C., LeGouët, J. L., Picqué, J. L., Carré, B., and Koch, P. M. (1985). *Phys. Rev. Lett.* **12**, 1281.

Bruhn, R., Schmidt, E., Schröder, H., and Sonntag, B. (1982). *J. Phys.* B **15**, 2807.

Chanderis, D., Guillot, C., Chauvin, G., Le Cante, J., and Petroff, Y. (1981). *Phys. Rev. Lett.* **47**, 1273.

Cherepkov, N. A. (1978). *Phys. Lett.* A **66**, 204.

Codling, K., West, J. B., Parr, A. C., Dehmer, J. L., and Stockbauer, R. L. (1980). *J. Phys.* B **13**, L693.

Connerade, J. P. (1983). *J. Phys.* B **16**, L329.

Crasemann, B., and Wuilleumier, F. (1985). *In* 'Atomic Innershell Physics' (Ed. B. Crasemann), p. 281 (Plenum: New York).
Dehmer, J. L., and Dill, D. (1976). *Phys. Rev. Lett.* **37**, 1049.
Derenbach, H., Kossmann, H., Malutzki, R., and Schmidt, V. (1984). *J. Phys.* B **17**, 2781.
Derenbach, H., and Schmidt, V. (1984). *J. Phys.* B **17**, 83.
Ederer, D. L., Parr, A. C., West, J. B., Holland, D. M. P., and Dehmer, J. L. (1982). *Phys. Rev.* A **25**, 2006.
Fahlman, A., Carlson, T. A., and Krause, M. O. (1983). *Phys. Rev. Lett.* **50**, 1114.
Fahlman, A., Krause, M. O., Carlson, T. A., and Svensson, A. (1984). *Phys. Rev.* A **30**, 812.
Garvin, L. J., Brown, E. R., Carter, S. L., and Kelly, H. P. (1983). *J. Phys.* B **16**, L269.
Gerard, P., Bizau, J. M., Cubaynes, D., and Wuilleumier, F. J. (1986). (personal communication).
Heckenkamp, Ch., Schäfers, F., Schönhense, G., and Heinzmann, U. (1984). *Phys. Rev. Lett.* **52**, 421.
Heimann, P. A., Truesdale, C. M., Kerkhoff, H. G., Lindle, D. W., Ferrett, T. A., Bahr, C. C., Brewer, W. D., Becker, U., and Shirley, D. A. (1985). *Phys. Rev.* A **31**, 2260.
Heinzmann, U., and Schäfers, F. (1980). *J. Phys.* B **13**, L415.
Heinzmann, U. (1980). *J. Phys.* B **13**, 4367.
Huang, K. N., and Starace, A. F. (1980). *Phys. Rev.* A **19**, 2335.
Hussein, M. I. A., Holland, D. M. P., Codling, K., Woodruff, P. R., and Ishiguro, E. (1985). *J. Phys.* B **18**, 2817.
Johnson, W. R., and Cheng, K. T. (1979). *Phys. Rev.* A **20**, 978.
Johnson, W. R., Cheng, K. T., Huang, K.-N., and LeDourneuf, M. (1980). *Phys. Rev.* A **22**, 989.
Kobrin, P. H., Becker, U., Southworth, S., Truesdale, C. M., Lindee, D. W., and Shirley, D. A. (1982). *Phys. Rev.* A **26**, 842.
Kobrin, P. H., Heimann, P. A., Kerkhoff, H. G., Lindle, D. W., Truesdale, C. M., Ferrett, T. A., Becker, U., and Shirley, D. A. (1983). *Phys. Rev.* A **27**, 3031.
Kobrin, P. H., Southworth, S., Truesdale, C. M., Lindle, D. W., Becker, U., and Shirley, D. A. (1984). *Phys. Rev.* A **29**, 194.
Krause, M. O. (1975). *In* 'Atomic Innershell Processes', Vol. II (Ed. B. Crasemann), p. 33 (Academic: New York).
Krause, M. O. (1980). *In* 'Synchrotron Radiation Research' (Eds H. Winick and S. Doniach), Ch. 5 (Plenum: New York).
Krause, M. O. (1984). *At. Phys.* **9**, 414.
Krause, M. O., Carlson, T. A., and Fahlman, A. (1984). *Phys. Rev.* A **30**, 1316.
Krause, M. O., Carlson, T. A., and Woodruff, P. R. (1981). *Phys. Rev.* A **24**, 1374.
Krause, M. O., Cerrina, F., and Fahlman, A. (1983*a*). *Phys. Rev. Lett.* **50**, 1118.
Krause, M. O., Cerrina, F., Fahlman, A., and Carlson, T. A. (1983*b*). *Phys. Rev. Lett.* **51**, 2093.
Krause, M. O., Gerard, P., Fahlman, A., Carlson, T. A., and Svensson, A. (1986). *Phys. Rev.* A **33**, 3146.
Krause, M. O., Svensson, W. A., Carlson, T. A., Leroi, G., Ederer, D. E., Holland, D. M. P., and Parr, A. C. (1985). *J. Phys.* B **18**, 4096.
Lahiri, J., and Manson, S. T. (1982). *Phys. Rev. Lett.* **48**, 614.
Lindle, D. W., Ferrett, T. A., Becker, U., Kobrin, P. H., Truesdale, C. M., Kerkhoff, H. G., and Shirley, D. A. (1985). *Phys. Rev.* A **31**, 714.
Lindle, D. W., Heimann, P. A., Ferrett, T. A., Kobrin, P. H., Truesdale, C. M., Becker, U., Kerkhoff, H. G., and Shirley, D. A. (1986). *Phys. Rev.* A **33**, 319.
Lyon, I. C., Peart, B., West, J. B., Kingston, A. E., and Dolder, K. (1984). *J. Phys.* B **17**, L345.
Manson, S. T. (1976). *Adv. Electron. Electron Phys.* **41**, 73.
Manson, S. T. (1977). *Adv. Electron. Electron Phys.* **44**, 1.
Manson, S. T., Msezane, A., Starace, A. F., and Shahabi, S. (1979). *Phys. Rev.* A **20**, 1005.
Nunnemann, A., Prescher, Th., Richter, M., Schmidt, M., Sonntag, B., Wetzel, H. E., and Zimmermann, P. (1985). *J. Phys.* B **18**, L337.
Ong, W., and Manson, S. T. (1978). *J. Phys.* B **11**, L65.
Parpia, F. A., Johnson, W. R., and Radojevic, V. (1984). *Phys. Rev.* A **29**, 3173.
Prescher, Th., Richter, M., Schmidt, E., Sonntag, B., and Wetzel, H. E. (1986). *J. Phys.* B **19**, 1645.

Preses, J. M., Burkhardt, C. E., Corey, R. L., Earsom, D. L., Daulton, T. L., Garver, W. P., Leventhal, J. J., Msezane, A. Z., and Manson, S. T. (1985). *Phys. Rev.* A **32**, 1264.
Rosenberg, R. A., White, M. G., Thornton, G., and Shirley, D. A. (1979). *Phys. Rev. Lett.* **43**, 327.
Salomonson, S., Carter, S. L., and Kelly, H. P. (1985). *J. Phys.* B **18**, L149.
Samson, J. A. R. (1982). *In* 'Handbuch der Physik', Vol. XXXI (Ed. W. Mehlhorn), p. 123 (Springer: Berlin).
Samson, J. A. R., and Pareek, P. N. (1985). *Phys. Rev.* A **31**, 1470.
Schmidt, E. (1985). Ph.D. Thesis, Hamburg University.
Schmidt, E., Schröder, H., Sonntag, B., Voss, H., and Wetzel, H. E. (1985). *J. Phys.* B **18**, 79.
Schönhense, G., and Heinzmann, U. (1984). *Phys. Rev.* A **29**, 987.
Schönhense, G., Schäfers, F., Heckenkamp, Ch., Heinzmann, U., and Baig, M. A. (1984). *J. Phys.* B **17**, L771.
Sonntag, B., and Wuilleumier, F. (1983). *Nucl. Instrum. Methods* **208**, 735.
Southworth, S., Becker, U., Truesdale, C. M., Kobrin, P. H., Lindle, D. W., Owaki, S., and Shirley, D. A. (1983). *Phys. Rev.* A **28**, 261.
Starace, A. F. (1982). *In* 'Handbuch der Physik', Vol. XXXI (Ed. W. Mehlhorn), p. 1 (Springer: Berlin).
Svensson, W. A. (1985). Thesis KTH, Stockholm.
Svensson, W. A., Krause, M. O., Carlson, T. A., Radojevic, V., and Johnson, W. R. (1986). *Phys. Rev.* A **33**, 1024.
Wendin, G. (1982). AIP Conf. Proc., Vol. 94 (Ed. B. Crasemann), p. 495 (AIP: New York).
Wendin, G., and Ohno, M. (1976). *Phys. Scr.* **14**, 148.
Wendin, G., and Starace, A. F. (1983). *Phys. Rev.* A **28**, 3143.
West, J. B., Woodruff, P. R., Codling, K., and Houlgate, R. G. (1976). *J. Phys.* B **9**, 407.
White, M. G., Southworth, S. H., Kobrin, P., Poliakoff, E. D., Rosenberg, R. A., and Shirley, D. A. (1979). *Phys. Rev. Lett.* **43**, 1661.
Woodruff, P. R., and Samson, J. A. R. (1982). *Phys. Rev.* A **25**, 848.
Wuilleumier, F. J. (1981). *At. Phys.* **7**, 491.
Wuilleumier, F. J. (1982). AIP Conf. Proc., Vol. 94 (Ed. B. Crasemann), p. 615 (AIP: New York).
Wuilleumier, F. J., and Krause, M. O. (1974). *Phys. Rev.* A **10**, 242.
Yates, B. W., Tan, K. H., Coatsworth, L. L., and Bancroft, G. M. (1985). *Phys. Rev.* A **31**, 1529.
Yin, R. Y., and Pratt, R. A. (1985). *Phys. Rev.* A **32**, 225.

Manuscript received 13 February, accepted 10 June 1986